PNAS
www.pnas.org

Supplementary Information for

Chemosensory mechanisms of host seeking and infectivity in skin-penetrating nematodes

Spencer S. Gang, Michelle L. Castelletto, Emily Yang, Felicitas Ruiz, Taylor M. Brown, Astra S. Bryant, Warwick N. Grant, Elissa A. Hallem

Elissa Hallem
Email: ehallem@ucla.edu

This PDF file includes:

SI Materials and Methods
Figures S1 to S12
Tables S1 to S4
Captions for Movies S1 to S4
References for SI reference citations

Other supplementary materials for this manuscript include the following:

Movies S1 to S4

SI Materials and Methods

Ethics Statement

Gerbils were used as hosts to passage *S. stercoralis*. Rats were used as hosts to passage *S. ratti*. Hamsters were used as hosts to passage *A. ceylanicum*. Procedures and protocols for animal subjects were approved by the UCLA Office of Animal Research and Oversight (protocol #2011-060-23), which follows AAALAC standards and the *Guide for the Care and Use of Laboratory Animals*.

Maintenance of *Strongyloides stercoralis*

S. stercoralis strain UPD (originally provided by Dr. James Lok, University of Pennsylvania) was serially passaged in male and female Mongolian gerbils obtained from Charles River Laboratories. Gerbil infections were carried out by collecting *S. stercoralis* iL3s from fecal-charcoal cultures by Baermann apparatus as described (1). iL3s were cleansed of fecal debris by suspension in ~0.5% low-gelling-temperature agarose; iL3s that crawled out of the agarose were collected and washed in sterile 1x PBS 5 times. Gerbils were anesthetized with isoflurane and inoculated with ~2,000-2,250 iL3s suspended in 200 μL sterile 1x PBS by inguinal subcutaneous injection. After a 14-day pre-patency period, feces infested with *S. stercoralis* were collected by placing infected gerbils on wire cage racks overnight with wet cardboard lining the cage bottom to prevent the feces from desiccating. Fecal pellets were collected the next morning, softened with dH_2O, mixed in a 1:1 ratio with autoclaved charcoal granules (bone char from Ebonex Corp., Cat # EBO.58BC.04), and stored in 10-cm diameter x 20-mm height Petri dishes lined with filter paper moistened with dH_2O. *S. stercoralis*-infested feces were collected between days 14-45 after initial infection of gerbils. *S. stercoralis* free-living adults were collected by incubating fecal-charcoal cultures at 20°C for 48 hours, or at 25°C for 24 hours. Free-living adults were isolated using a Baermann apparatus. iL3s were collected by incubating fecal-charcoal cultures at 23°C for 6-14 days; iL3s were isolated using a Baermann apparatus.

Maintenance of *Strongyloides ratti*

S. ratti strain ED321 (originally provided by Dr. James Lok, University of Pennsylvania) was serially passaged in Sprague Dawley rats obtained from Envigo as described (2). Rat infections were carried out by collecting *S. ratti* iL3s from fecal-charcoal cultures using a Baermann apparatus. iL3s were washed in 1x PBS 5 times and rats were inoculated with ~800 iL3s in 300 μL sterile 1x PBS by subcutaneous injection. After a 7-day pre-patency period, feces infested with *S. ratti* were collected as described above. *S. ratti*-infested feces were collected between days 7-23 after initial infection. *S. ratti* free-living adults and iL3s were incubated and isolated using a Baermann apparatus as described above.

Maintenance of *Parastrongyloides trichosuri*

P. trichosuri (provided by Dr. Warwick Grant, La Trobe University) was a mixed population of wild isolates collected from the feces of wild *Trichosurus vulpecula* brushtail possums near Hunterville, New Zealand and urban possums in Kioloa, New South Wales, Australia. *In vitro* cultures of free-living *P. trichosuri* were maintained as described, with modifications (3, 4). Briefly, 6 cm Nematode Growth Media (NGM) plates with *E. coli* OP50 were prepared using standard methods (5). For optimal *P. trichosuri* growth, 3% agar plates were used to limit nematode penetration into the agar and $1/10^{th}$ the standard peptone was added to the NGM media. For each plate, an autoclaved fecal pellet collected from New Zealand white rabbits

was deposited in the center of the NGM plate on the OP50 lawn. The fecal pellet was punctured, saturated with OP50 solution, and allowed to dry overnight. The next day, *P. trichosuri* free-living cultures containing all life stages were pipetted onto the OP50-saturated feces (~100-200 nematodes per plate). The free-living cultures were maintained at room temperature and passaged every 3-4 days by pouring BU saline (6) into the plate and floating nematodes off the bacterial lawn and fecal pellet. The nematodes were washed 5 times in BU saline and pipetted onto fresh NGM + OP50 plates supplemented with OP50-saturated autoclaved rabbit feces. *P. trichosuri* free-living adults were collected by transferring BU-washed nematodes to a watch glass; after the adults gravity-settled to the bottom of the dish, other life stages were removed in the supernatant. *P. trichosuri* iL3s were collected by removing nematode-infested rabbit feces from NGM plates and preparing 6 cm fecal charcoal cultures as described above. Fecal-charcoal cultures were incubated at 23°C and iL3s were collected 7-21 days later using a Baermann apparatus.

Maintenance of *Ancylostoma ceylanicum*

A. ceylanicum Indian strain, US National Parasite Collection Number 102954 (provided by Dr. John Hawdon, George Washington University) was serially passaged in male and female Syrian golden hamsters from Envigo as described (7). Hamster infections were carried out by collecting *A. ceylanicum* iL3s from fecal-charcoal cultures using a Baermann apparatus. iL3s were washed in sterile ddH_2O and hamsters were inoculated with ~70-100 iL3s in 100 μL sterile water by oral gavage. After a 14-day pre-patency period, feces infested with *A. ceylanicum* were collected as described above. *A. ceylanicum*-infested feces were collected between days 14-44 after initial infection. *A. ceylanicum* iL3s were collected by incubation of fecal-charcoal cultures at 23°C for 14-21 days and isolated using a Baermann apparatus.

Maintenance of *Caenorhabditis elegans*

C. elegans dauers used to examine the relationship between nictation frequency and body length were from the wild isolate CB4856 (“Hawaii”). *C. elegans* were maintained on NGM plates seeded with *E. coli* OP50 using standard methods (5). Dauer larvae were collected from the lids of plates where the nematodes had depleted all of the OP50. Dauers were stored in dH_2O at room temperature prior to use, and were used within 2 weeks of collection.

Host odorant and fecal odor assays

Odorant assays were performed on 9 cm chemotaxis plates (8) as described (2). Populations of ~100-400 free-living adults or iL3s (~100-200 for *S. stercoralis, S. ratti,* and *P. trichosuri* adults; ~100-200 for *S. stercoralis* and *P. trichosuri* iL3s; ~300-400 for *S. ratti* iL3s; and ~200-300 for *A. ceylanicum* iL3s) were spread vertically along the center of the plate. For odorant chemotaxis assays, 5 μL of host odorant or control (paraffin oil, ddH_2O, or ethanol), was then pipetted on each side of the plate in the center of a 2 cm diameter scoring region. The scoring regions were aligned horizontally along the center of the plate with the odorants placed 1 cm from the edge of the plate (*SI Appendix,* Fig. S1). For fecal chemotaxis assays, feces were obtained from an overnight fecal collection. Feces were moistened to a paste with ddH_2O. 1 cm radius circles of filter paper were affixed to the lid of a chemotaxis plate above each scoring region using double-stick tape. 0.25 g fecal paste was placed onto one of the filter-paper circles, and 50 μL ddH_2O was pipetted onto the other circle.

For both odorant and fecal chemotaxis assays, the worms were allowed to crawl undisturbed in the odorant gradient for 3 hours at room temperature on a vibration-insulating platform. The chemotaxis index (CI) was calculated as: CI = (# worms in odorant scoring region - # worms in control scoring region) / (# worms in both scoring regions). CI values range from +1 to -1, with a positive CI indicating attraction to the tested odorant and a negative CI indicating repulsion from the odorant. Adult assays were performed with odorants diluted 1:10 in either paraffin oil, ddH_2O, or ethanol. iL3 assays were performed with undiluted odorant. For *S. stercoralis*, in instances where significantly different responses to a host odorant were observed between free-living adults and iL3s, we also tested iL3s using 1:10 dilutions of odorant (*SI Appendix,* Fig. S5). These assays confirmed that the observed changes in chemosensory responses were the result of life-stage-specific changes in olfactory preferences and not the result of odorant concentration. To account for directional bias, two identical chemotaxis assays were performed simultaneously with the test odorant placed in scoring regions on opposite sides. All assays where the absolute difference in CI for the two plates was $\geq$0.9 were discarded. Assays were also discarded if <7 total worms (or <8 total worms for *A. ceylanicum* assays) moved into the scoring regions on one or both of the paired plates. Details on preparation of odorants, and diluents for each odorant, are described in *SI Appendix,* Table S1. Chemotaxis assays with odor from animal feces were performed essentially as described (2, 7). Gerbil, dog, rat, hamster, and rabbit feces were collected fresh the morning of assays from the bottoms of cages housing uninfected animals. Possum feces were collected from uninfected *T. vulpecula* housed at La Trobe University in Melbourne, Australia and stored at -20°C until assays were performed, at which point the fecal pellets were warmed to room temperature and prepared for assays as described (2, 7). For all chemotaxis assays, each trial involved a distinct population of worms; in no instance was the same population of worms used for multiple assays. Moreover, all trials were conducted across multiple days to control for day-to-day variability during assays.

Fecal dispersal assays

Fecal dispersal assays were performed essentially as described (7). Fresh fecal pellets were collected from the bottoms of cages housing uninfected animals on the morning of assays. For fecal dispersal assays using host feces (Fig. 3 and *SI Appendix*, Fig. S7a), gerbil feces were used for *S. stercoralis* and hamster feces were used for *A. ceylanicum*. For fecal dispersal assays using non-host feces (*SI Appendix,* Fig. S7b), rat feces were used for both *S. stercoralis* and *A. ceylanicum*. For all assays, ~0.035 g of feces was placed in the center of a chemotaxis plate and 14-35 iL3s were pipetted onto the feces in <5 μL of dH_2O. The plates were left undisturbed for 1 hour (Fig. 3 and *SI Appendix,* Fig. S7b) or 3 hours (*SI Appendix,* Fig. S7a) on a vibration-reducing platform. The number of iL3s remaining on feces, off feces but in a 4 cm diameter area around the feces (zone 1), or off feces and outside the 4 cm diameter area around the feces (zone 2) were counted as shown in Fig. 3a. iL3s that were stuck to and therefore trapped on the plate walls and lid were counted as part of zone 2. Since iL3s on the feces were not visible, the number of iL3s on feces was counted by subtracting the number of iL3s in zones 1 and 2 from the total number of iL3s plated at the beginning of the assay. For all dispersal assays, each trial involved a distinct population of worms; in no instance was the same population of worms used for multiple assays. Moreover, all trials were conducted across multiple days to control for day-to-day variability during assays.

Nictation assay

Nictation assays were performed as described with modifications (7, 9). Briefly, PDMS molds with near-microscopic pillars that reduce surface tension and allow iL3s to stand were used to cast chips made from 4% agar dissolved in ddH_2O. Agar poured over the PDMS mold was allowed to solidify and the agar chip was then separated from the mold and placed at 37˚C for 2 hours to dry. The agar chip was then cooled at room temperature for at least 1 hour before assays were performed. A 5 μL drop of dH_2O containing 10-35 iL3s was pipetted onto the center of the agar chip. Once the dH_2O dried, the iL3s were left for 10 minutes to acclimate to the agar chip. Individual iL3s were then observed for a 2-minute period. If at any point during the 2 minutes the iL3 raised at least half of its body from the plate for at least 5 seconds, it was counted as nictating (Fig. 3c). The process was then repeated for other iL3s on the same agar chip. For *A. ceylanicum* iL3s, chips were approximately 3 cm x 3.5 cm in size. For *S. stercoralis* iL3s, larger chips of approximately 8 cm x 4 cm were used since these iL3s frequently crawled off smaller chips during the 10-minute acclimation period. For *C. elegans* dauers (*SI Appendix,* Fig. S8), nictation assays were conducted on 5% agar. Nictation assays were conducted across multiple days to control for day-to-day variability in assay conditions. To examine the correlation between body length and nictation frequency (*SI Appendix,* Fig. S8), *S. stercoralis*, *S. ratti*, and *A. ceylanicum* iL3s were anesthetized with 50 mM levamisole and then mounted on a slide with 5% Noble agar dissolved in BU saline. DIC images were taken using a Zeiss AxioImager A2 microscope. Body length measurements were obtained from the images using ImageJ.

CRISPR/Cas9-mediated targeted mutagenesis of *Ss-tax-4*

Targeted mutagenesis of the *S. stercoralis tax-4* gene (SSTP_0000981000) was performed as previously described using the same CRISPR target site (GTAACATTTGACTTGATGGGTGG) (10, 11). *Ss-tax-4* was identified based on sequence homology with *C. elegans tax-4*; the *Ss-tax-4* gene was also predicted as an ortholog of *Ce-tax-4* on WormBase ParaSite (12). The CRISPR target site and gRNA were selected using Geneious 9 software (13). gRNA design parameters used for optimized CRISPR/Cas9 mutagenesis in *C. elegans* were similarly used for *S. stercoralis* (14, 15). The single guide RNA (sgRNA) expression construct targeting *Ss-tax-4* (pMLC47) was synthesized by GENEWIZ (South Plainfield, New Jersey) to include 500 bp of the *S. ratti* U6 promoter and 277 bp of the *S. ratti* U6 3'UTR flanking the *Ss-tax-4* sgRNA. For homology-directed repair at *Ss-tax-4*, a construct (pEY11) was made by subcloning 539 bp 5' and 671 bp 3' homology arms flanking the *Ss-tax-4* CRISPR site into the *Ss-act-2::mRFPmars* vector pAJ50, which drives *mRFPmars* expression in the nematode body wall (*SI Appendix,* Fig. S10) (10, 16). Cas9 endonuclease was expressed from the vector pPV540, in which *Strongyloides*-codon-optimized Cas9 expression is driven by the *S. ratti eef-1A* promoter (10). The pMLC47, pEY11, and pPV540 vectors were mixed and microinjected into the syncytial gonad of free-living adult females. F_1 iL3 progeny were screened for potential *Ss-tax-4* disruptions as described below. Microinjections were done with either 100 ng/μL or 200 ng/μL total DNA using the following recipes: 60 ng/μL pMLC47, 20 ng/μL pEY11, and 20 ng/μL pPV540 or 80 ng/μL pMLC47, 80 ng/μL pEY11, and 40 ng/μL pPV540. No-Cas9-control injections were performed using the same recipes but with pPV540 omitted from the mix. A plasmid summary is provided in *SI Appendix,* Table S3. Primers used to amplify the *Ss-tax-4* homology arms from *S. stercoralis* gDNA are provided in *SI Appendix*, Table S4. The gene structure diagrams

for *C. elegans* and *S. stercoralis tax-4* shown in *SI Appendix,* Fig. S10 were generated with Exon-Intron Graphic Maker (Version 4, www.wormweb.org).

Microinjection of *S. stercoralis*

Microinjection of syncytial gonads of *S. stercoralis* free-living adult females was performed using standard methods from *C. elegans* and *Strongyloides* species, with modifications (10, 16, 17). Briefly, microinjected females were recovered from injection slides and transferred to 6 cm 2% NGM plates seeded with OP50; wild-type free-living males were added to the plate for mating. After a minimum recovery time of 30 minutes on NGM, the plate was flooded with ddH_2O and all worms were pipetted onto 6 cm fecal-charcoal plates made with fresh gerbil feces from uninfected animals, collected and prepared as described above. Fecal-charcoal cultures were maintained at 23°C for 6-14 days to collect F_1 iL3s.

Selection of *Ss-tax-4* iL3s

iL3 progeny from microinjected females were recovered using a Baermann apparatus and stored in ~2 mL of BU saline in a watch glass. To screen for *mRFPmars* expression, ~15-20 μL of iL3s in BU saline (~100 worms) were pipetted onto a 6 cm 2% NGM plate seeded with OP50. Freely crawling iL3s were screened for *mRFPmars* expression under a Leica M165 FC fluorescence microscope. *mRFPmars*-expressing iL3s were picked into a small watch glass with ~1 mL of BU saline for storage prior to assays. The fluorescent iL3s collected for behavioral experiments and subsequent genotyping were selected based on expression of *mRFPmars* along the full body wall of the iL3 (10). iL3s with patchy or faint *mRFPmars* expression were not collected, as these iL3s were unlikely to have complete CRISPR/Cas9-mediated HDR at both target alleles, as described in Gang *et al.,* 2017 (10). A summary of free-living adult microinjections and iL3 screening for *Ss-tax-4* can be found in *SI Appendix,* Table S2.

***In vitro* activation assays**

In vitro activation assays for skin-penetrating iL3s were performed as described (18), with modifications. For the population assays shown in Fig. 5c and *SI Appendix,* Fig. S11-12, iL3s were collected using a Baermann apparatus, washed 3 times in BU saline in 15 mL conical tubes, and pelleted by centrifugation. Pelleted iL3s were then resuspended in 10 mL of BU saline supplemented with 100 μL of 100x penicillin-streptomycin (10,000 U/mL, Gibco 15140-122), 100 μL of 100x amphotericin B (250 μg/mL, Gibco 15290-018), and 10 μL of 1000x tetracycline hydrochloride dissolved in ddH_2O (5 mg/mL, Sigma-Aldrich T7660-5G). iL3s were axenized for 3 hours in the antibiotic solution, in the dark, at room temperature. The iL3s were then pelleted by centrifugation and the supernatant was removed. 5 μL of the pellet containing ~100-200 iL3s was then transferred to one well of a 96-well plate containing 110 μL DMEM. Typically, iL3s were aliquoted to 6-12 wells containing DMEM, per condition, per assay. The 96-well plate was then transferred to a tissue culture incubator set to the desired experimental conditions: 37°C and 5% CO_2, 25°C and 5% CO_2, or 37°C and 0% CO_2. iL3s were incubated for 21 hours, after which 2.5 μL of fluorescein isothiocyanate (FITC, 20mg/mL in N,N-dimethylformamide, Acros Organics 119252500) was added to each well. The iL3s were then returned to the culture conditions for 3 hours. Wells containing iL3s were pipetted into a 15 mL conical tube filled with BU saline. The iL3s were washed 5 times with BU saline to remove excess FITC on the outer cuticle of the worms. They were then transferred to a chemotaxis plate and paralyzed by applying a solution of 1% nicotine (Sigma-Aldrich N3876) in ddH_2O.

The iL3s were screened using a Leica M165 FC fluorescence microscope for the presence of FITC in the pharynx, which is indicative of the resumption of feeding that occurs during activation. The percentage of activated iL3s was calculated as: (# FITC-positive iL3s) / (total # iL3s scored). For all activation assays, each trial involved a distinct population of worms; in no instance was the same population of worms used for multiple assays. Moreover, all trials were conducted across multiple days to control for day-to-day variability during assays.

For the dispersal assay to compare the motility of non-activated vs. activated iL3s in *SI Appendix*, Fig. S11, the non-activated control iL3s were incubated in BU saline in the absence of applied CO_2 at room temperature, while activated iL3s were incubated in DMEM with 5% CO_2 and 37°C. After 24 hours, iL3s from each condition were then tested in a 1-hour dispersal assay at room temperature, as described above for fecal dispersal assays except in the absence of feces. To confirm activated iL3s had indeed activated and control iL3s had not activated, a subset of iL3s for each condition were incubated in parallel but stained with FITC and scored as described above.

For *in vitro* activation assays on single wild-type, no-Cas9-control, or *Ss-tax-4* iL3s, as shown in Fig. 5d, the procedure was modified such that each iL3 was axenized in 110 μL of BU saline supplemented with antibiotics in its own well in a 96-well plate. Each iL3 was then pipetted into its own well containing 110 μL of DMEM and was incubated as described above. Each iL3 recovered from incubation and FITC staining was washed by pipetting up and down in a watch glass filled with ~2 mL dH_2O. The iL3s were then transferred to a chemotaxis plate, paralyzed in 1% nicotine solution, scored for activation, and collected for gDNA isolation as described below. Experiments were conducted across multiple days to control for day-to-day variability in assay conditions.

Media preparation for *in vitro* activation assays

To assess the requirement for 37°C and 5% CO_2 for iL3 activation, shown in Fig. 5c and *SI Appendix,* Fig. S12, we prepared DMEM without sodium bicarbonate to ensure that the only source of CO_2 or HCO_3^- was supplied by the tissue culture incubator. To prepare sodium-bicarbonate-free DMEM, we added 0.4044 g DMEM powder (4.5 g/L glucose, L-glutamine & sodium pyruvate without sodium bicarbonate, Corning 50-003-PB) to 30 mL of ddH_2O. 300 μL of penicillin-streptomycin, 300 μL of amphotericin B, and 30 μL of tetracycline-HCl was added, as described above, to inhibit growth of bacterial and fungal spores transferred with iL3s from fecal-charcoal plates. As an alternative buffering agent to sodium bicarbonate, 0.1788 g HEPES (25 mM final concentration, Fisher BP310-100) was added to the solution. For 37°C and 5% CO_2, and 25°C and 5% CO_2 assay conditions, the room temperature pH was titrated to ~7.6-7.7 with 5 M NaOH. For the 37°C and 0% CO_2 condition, the room temperature pH was titrated to ~7.0 and 2 M sodium gluconate was added to balance the molar ratio of Na^+ with the 5% CO_2 conditions. The DMEM solutions were filter-sterilized through a 0.22 μm membrane (Millipore Millex-GV SLGV033RS) connected to a Luer-Lok syringe into a sterile 50 mL conical tube. 110 μL aliquots were pipetted into individual wells of a 96-well plate, as described above. The 96-well plate was incubated in the desired heat and % CO_2 for at least 1 hour. Following 1 hour of incubation, the pH of the media was checked to ensure pH ~7.0 prior to adding iL3s for overnight incubation. For testing iL3s in the standard 37°C and 5% CO_2 condition (Fig. 5d and *SI Appendix*, Fig. S11), standard DMEM media with sodium bicarbonate was used (4.5 g/L glucose, L-glutamine & sodium pyruvate, Corning 10-013-CV).

Single iL3 genotyping

To extract genomic DNA from individual *S. stercoralis* iL3s, we followed the previously described procedure (10). A single iL3 was transferred to a PCR tube containing 5-6 μL of nematode lysis buffer (50 mM KCl, 10 mM Tris pH 8, 2.5 mM $MgCl_2$, 0.45% Nonidet-P40, 0.45% Tween-20, 0.01% gelatin in dH_2O) supplemented with ~0.12 μg/μL Proteinase-K and ~1.7% 2-mercaptoethanol. Tubes were placed at -80°C for at least 20 min, then transferred to a thermocycler for digestion: 65°C (2 h), 95°C (15 min), 10°C (hold). For long-term storage, iL3s were left undigested at -80°C and thermocycler digestion was performed the day of PCR-genotyping. To genotype wild-type iL3s, no-Cas9-control iL3s, or *Ss-tax-4* iL3s, PCR reactions were performed with GoTaq G2 Flexi DNA Polymerase (Promega, Cat. # M7801) or Herculase II Fusion DNA Polymerase (Agilent Cat. # 600675) using the following thermocycler conditions: denature 95°C (2 min); PCR 95°C (30 s), 55°C (30 s), 72°C (1 min) x 35 cycles; final extension 72°C (5 min); 10°C (hold). The 5-6 μL single iL3 gDNA preparation was split evenly across control, wild-type locus, 5' integration, and 3' integration reactions, as shown in *SI Appendix,* Fig. S10. Primer sets used for *Ss-tax-4* genotyping can be found in *SI Appendix,* Table S4. Quantification of PCR products was performed with a ChemiDoc MP Imaging System (Bio-Rad) using the Image Lab Version 5.1 Relative Quantity Tool as previously described (10).

Fluorescent microscopy

Fluorescent microscopy was performed essentially as described (10, 11). Activated, nicotine-paralyzed iL3s were collected from chemotaxis plates and were pipetted onto a 5% Noble agar pad dissolved in ddH_2O. The slide was mounted under a Zeiss AxioImager A2 microscope and epifluorescence images were taken with a Zeiss Axiocam camera. Images were processed using Zeiss AxioVision software.

Statistical analysis

All standard statistical analysis was performed using GraphPad Prism version 8.3.0, GraphPad Software, La Jolla, California, USA (www.graphpad.com). The standard statistical tests used for each experiment are described in the figure captions. For all data sets, the D'Agostino-Pearson omnibus normality test was used to determine if values came from a Gaussian distribution. For data sets that were normally distributed, parametric tests were used. For non-normal distributions, non-parametric tests were used. Power analyses, where described below, were performed using G*Power version 3.1.9.3 (19). The heatmaps shown in Fig. 1c and Fig. 2c were generated using Heatmapper (www.heatmapper.ca) with individual chemotaxis index scores as input values. Heatmapper was also used for the hierarchical clustering of odorants based on Euclidean distance with average linkage as the clustering method (20). The behavioral dendrogram shown in Fig. 1d was constructed using PAST version 3.11 with hierarchical clustering using the Unweighted Pair Group Method with Arithmetic Mean (UPGMA) (21). For Fig. 1e-f and Fig. 2d-e, significance values are for the responses to each odorant for the full odorant panel compared to the paraffin oil control. For all species and life stages, ethanol and ddH_2O control responses were not significantly different from paraffin oil control responses; thus, paraffin oil was used as the control for all odorant panels (*SI Appendix,* Fig. S1). Sample sizes for single-iL3 assays were determined using a Z-test for independent proportions (tails = 2, $\alpha = 0.05$, Power = 0.90).

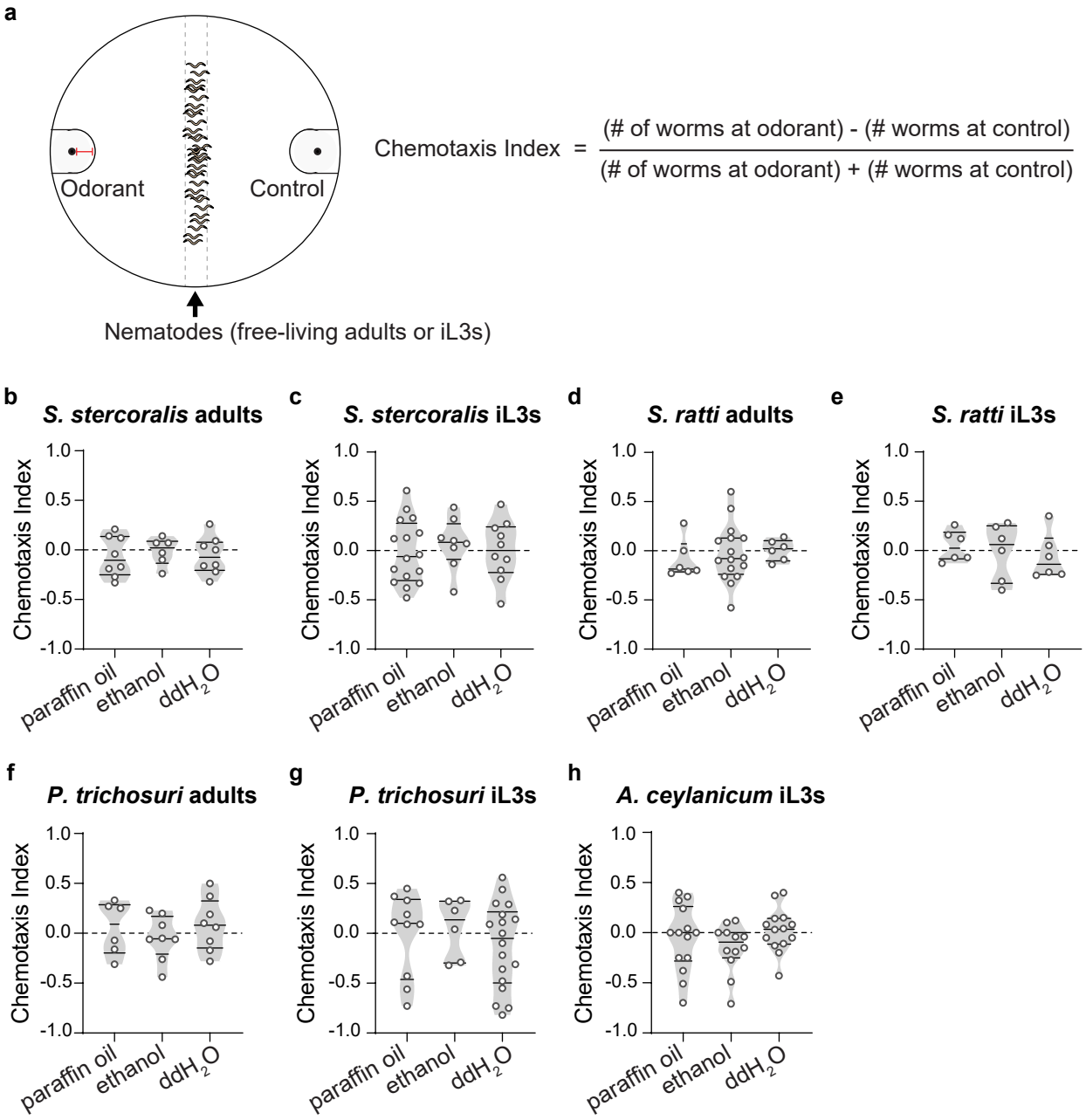

Fig. S1. Nematode chemotaxis assay. a. Each nematode species and life stage (free-living adults or iL3s) was assayed using the same format. Nematodes were spread vertically along the center of the plate. Odorant and control were placed on each side of the plate (black dots). The nematodes were allowed to migrate in the odorant gradient for 3 hours. The number of animals in the scoring regions (extended circles around the black dots) was counted. The chemotaxis index was then calculated as shown. The chemotaxis index ranges from +1 to -1, with positive values indicating attraction to the host odorant and negative values indicating repulsion from the host odorant. Red scale bar = 1 cm. **b-h.** Control chemotaxis assays for each species and life stage, where the indicated control was placed on both sides of the plate. For each species and life stage, responses to paraffin oil, ethanol, and ddH_2O controls were approximately neutral (chemotaxis index of ~0.0) and were not significantly different from each other (Kruskal-Wallis test). n = 6-18 trials for each odorant and life stage combination. Each dot represents an individual chemotaxis assay. Lines indicate medians and interquartile ranges.

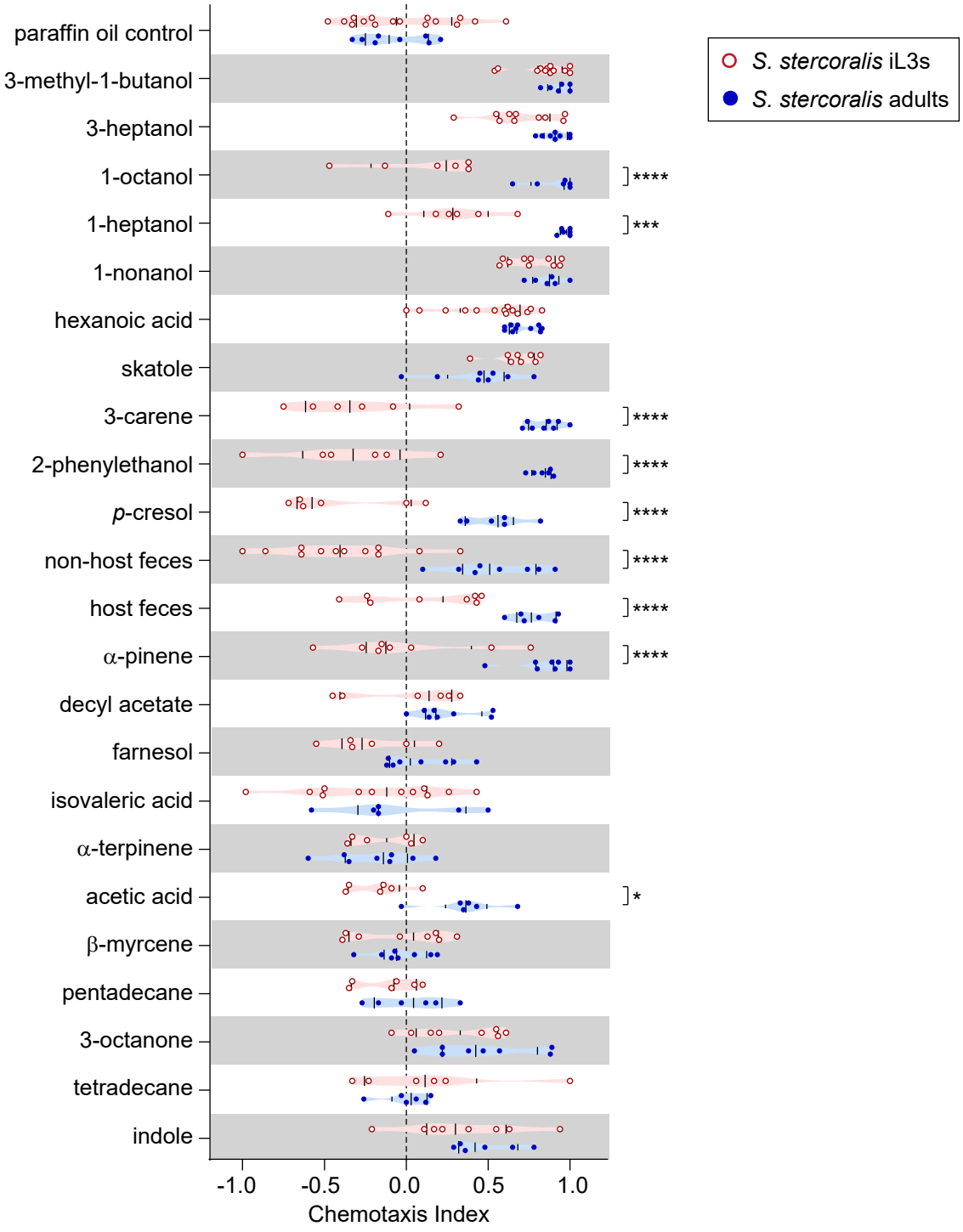

Fig. S2. *S. stercoralis* free-living adults and iL3s respond differently to a subset of odorants from the mammalian odorant panel. 1-octanol, 1-heptanol, 3-carene, 2-phenylethanol, *p*-cresol, non-host feces, host feces, α-pinene, and acetic acid were more attractive to free-living adults than iL3s. Sources of host and non-host feces, respectively, for *S. stercoralis* fecal odor assays = dogs, rats. **P*<0.05, ****P*<0.001, *****P*<0.0001, two-way ANOVA with Sidak's post-test. n = 6-16 trials for each odorant and life stage combination. Each dot represents an individual chemotaxis assay. Lines indicate medians and interquartile ranges. These data are also depicted in Fig. 1 and 2.

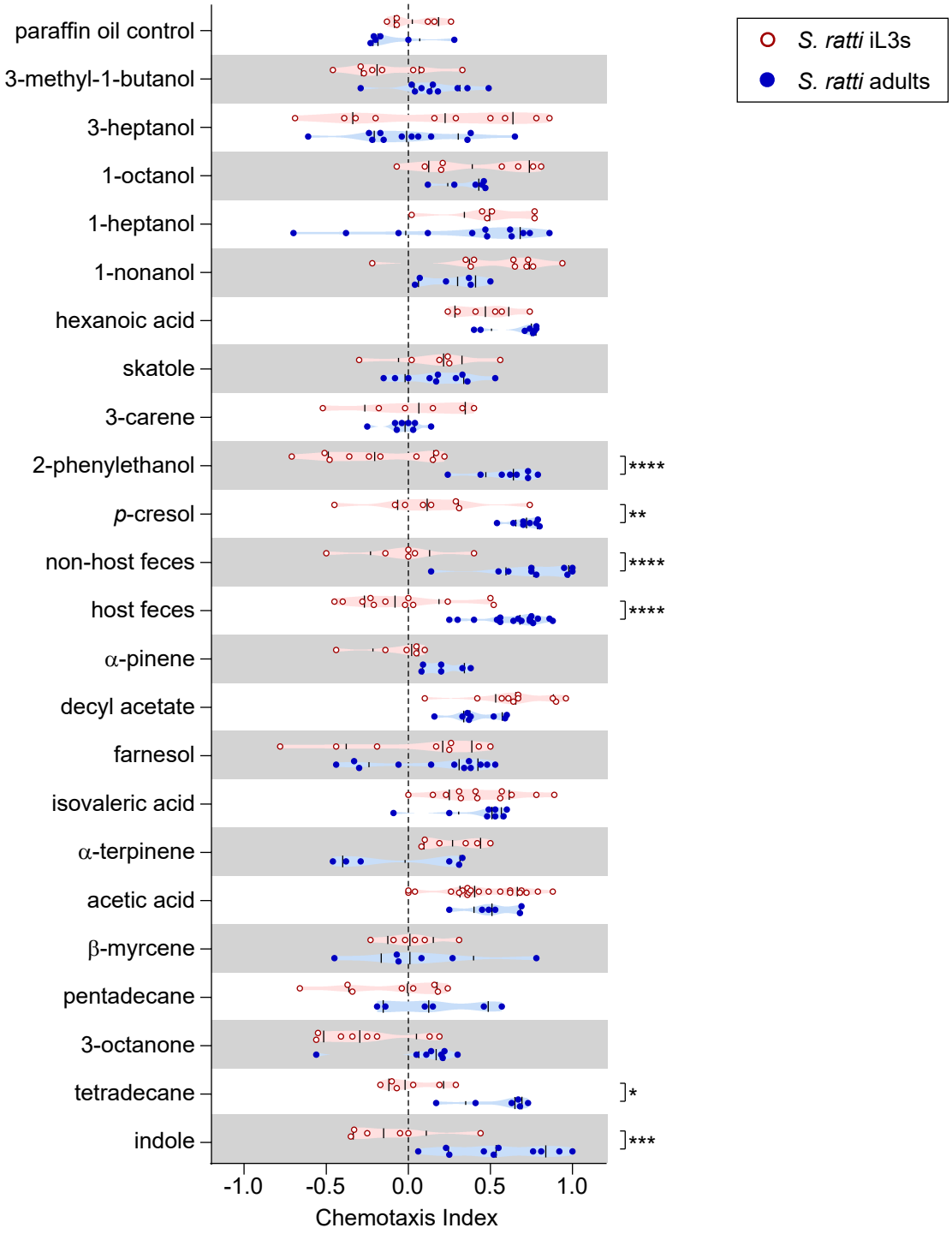

Fig. S3. *S. ratti* free-living adults and iL3s respond differently to a subset of odorants from the mammalian odorant panel. 2-phenylethanol, *p*-cresol, non-host feces, host feces, tetradecane, and indole were more attractive to free-living adults than iL3s. Sources of host and non-host feces, respectively, for *S. ratti* fecal odor assays = rats, dogs. **P*<0.05, ***P*<0.01, ****P*<0.001, *****P*<0.0001, two-way ANOVA with Sidak's post-test. n = 6-20 trials for each odorant and life stage combination. Each dot represents an individual chemotaxis assay. Lines indicate medians and interquartile ranges. These data are also depicted in Fig. 1.

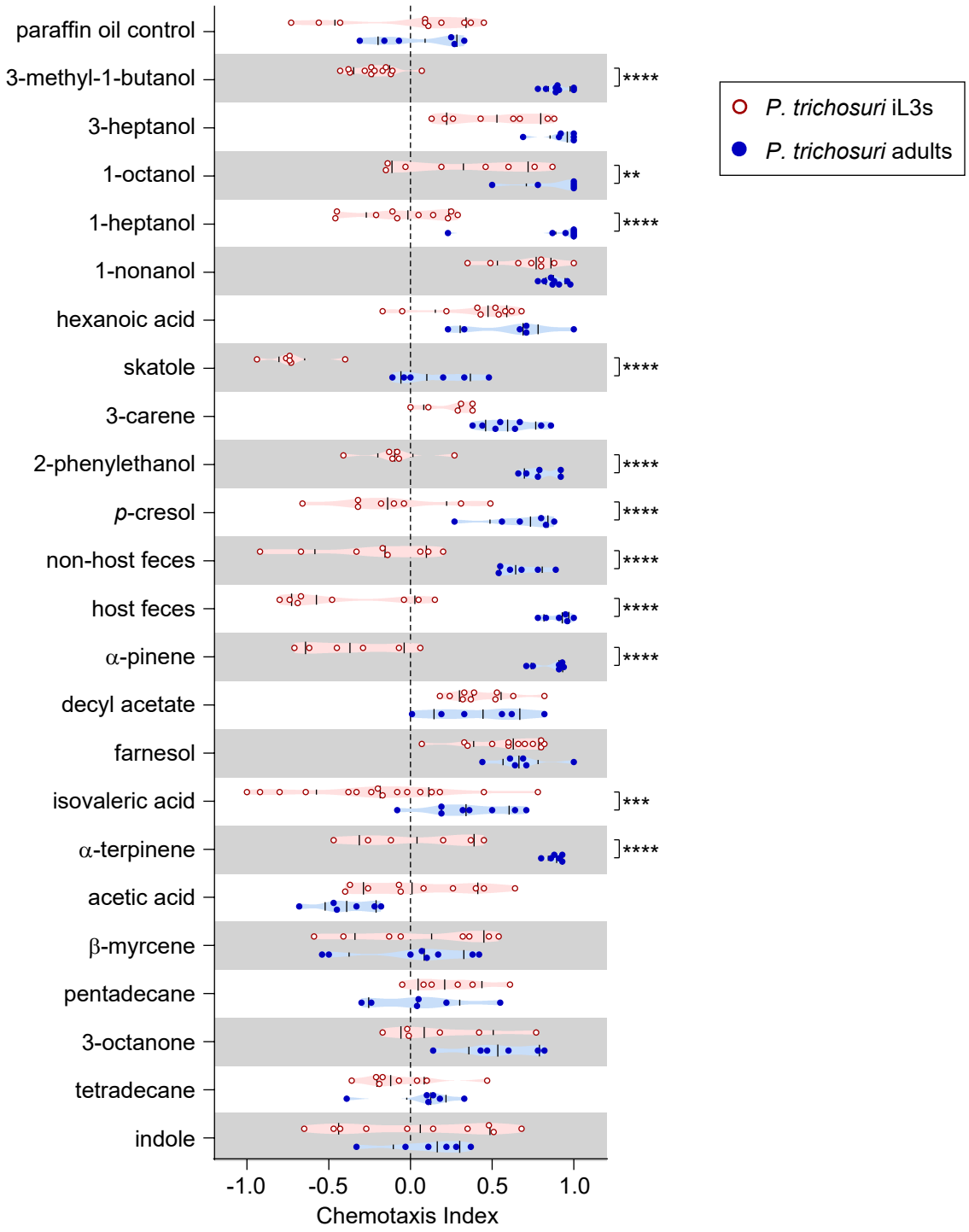

Fig. S4. *P. trichosuri* free-living adults and iL3s respond differently to a subset of odorants from the mammalian odorant panel. 3-methyl-1-butanol, 1-octanol, 1-heptanol, skatole, 2-phenylethanol, *p*-cresol, non-host feces, host feces, α-pinene, isovaleric acid, and α-terpinene were more attractive to free-living adults than iL3s. Sources of host and non-host feces, respectively, for *P. trichosuri* fecal odor assays = brushtail possums, rats. ***P*<0.01, ****P*<0.001, *****P*<0.0001, two-way ANOVA with Sidak's post-test. n = 6-16 trials for each odorant and life stage combination. Each dot represents an individual chemotaxis assay. Lines indicate medians and interquartile ranges. These data are also depicted in Fig. 1.

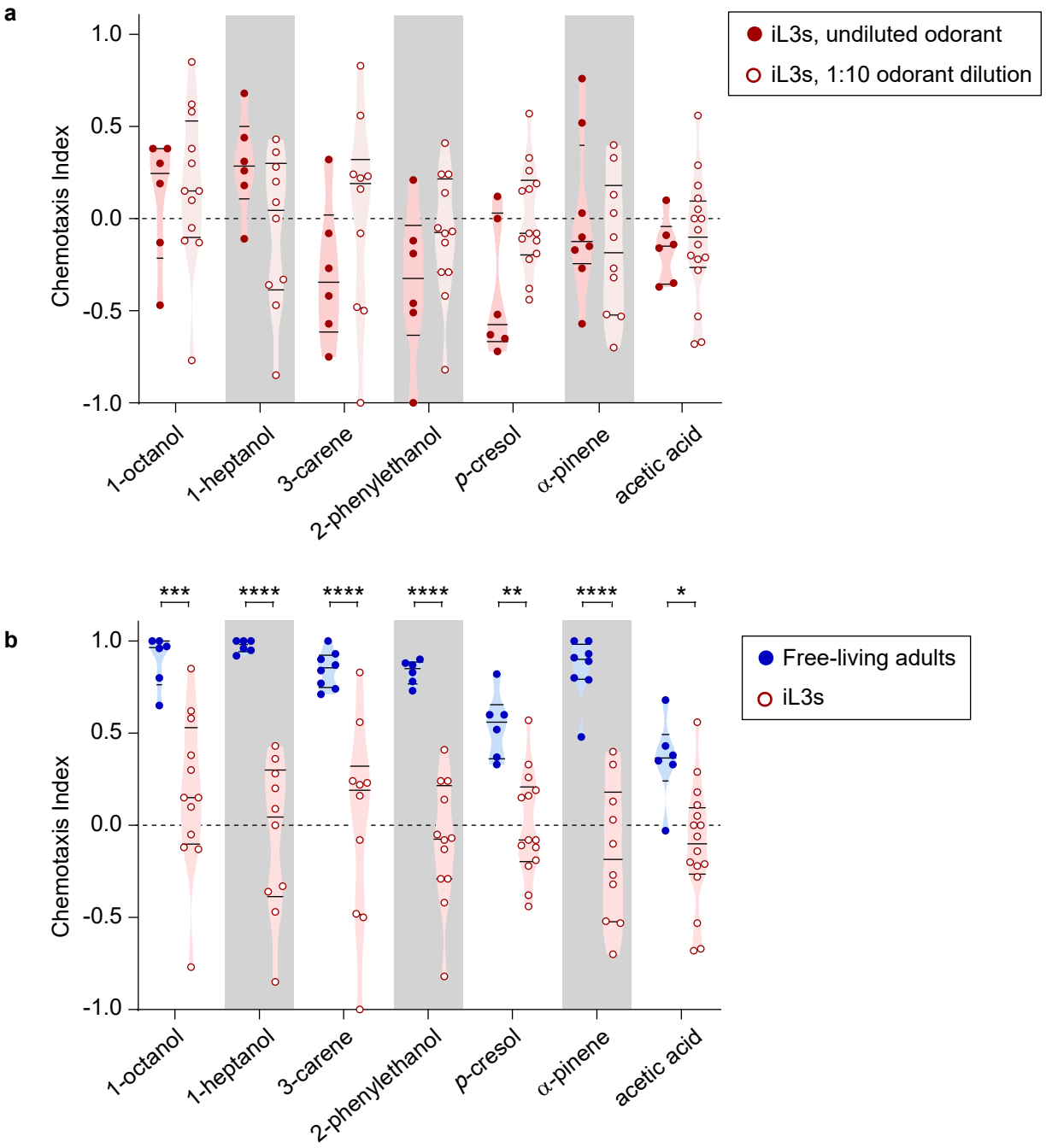

Fig. S5. Responses of *S. stercoralis* iL3s to different concentrations of mammalian odorants. **a.** The responses of *S. stercoralis* iL3s to selected odorants were similar when odorants were undiluted or diluted 1:10. P=0.253, two-way ANOVA. n = 6-16 trials for each odorant and concentration combination. **b**. *S. stercoralis* free-living adults and iL3s respond differently to a subset of odorants from the mammalian odorant panel when both life stages are tested with 1:10 dilutions of odorants. *P<0.05, **P<0.01, ***P<0.001, ****P<0.0001, two-way ANOVA with Sidak's post-test. n = 6-16 trials for each odorant and life stage combination. Each dot represents an individual chemotaxis assay. Lines indicate medians and interquartile ranges. Odorants tested here were selected because they yielded significant responses in *SI Appendix,* Fig. S2. Data for undiluted odorant responses are also depicted in Fig. 1 and 2.

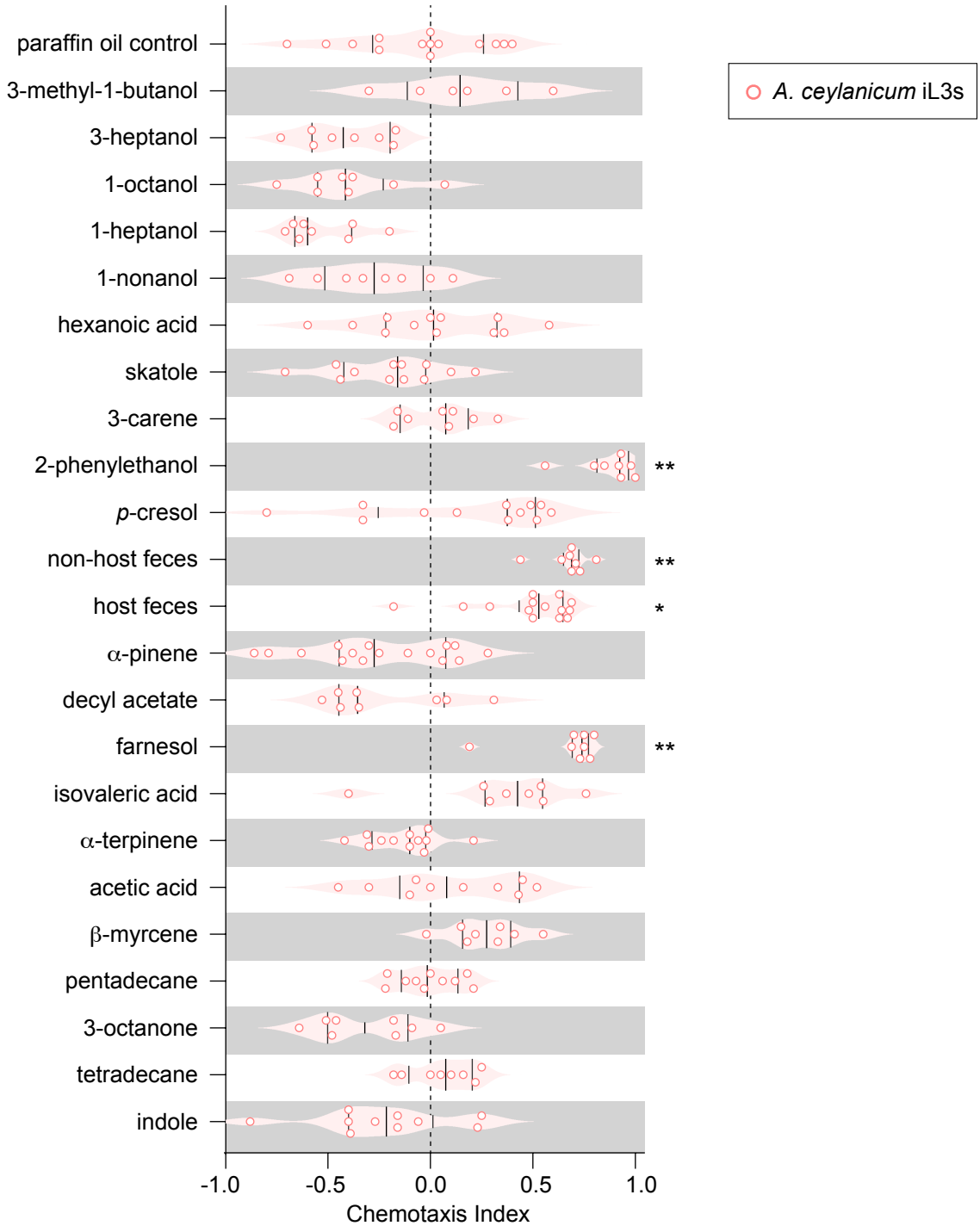

Fig. S6. Responses of *A. ceylanicum* iL3s to the mammalian odorant panel. 2-phenylethanol, non-host feces, host feces, and farnesol were attractive for iL3s. Sources of host and non-host feces, respectively, for *A. ceylanicum* fecal odor assays = hamsters, gerbils. *P<0.05, **P<0.01. n = 6-16 trials for each odorant. Significant responses were calculated relative to the paraffin oil control, Kruskal-Wallis test with Dunn's post-test. Each dot represents an individual chemotaxis assay. Lines indicate medians and interquartile ranges. These data are also depicted in Fig. 2.

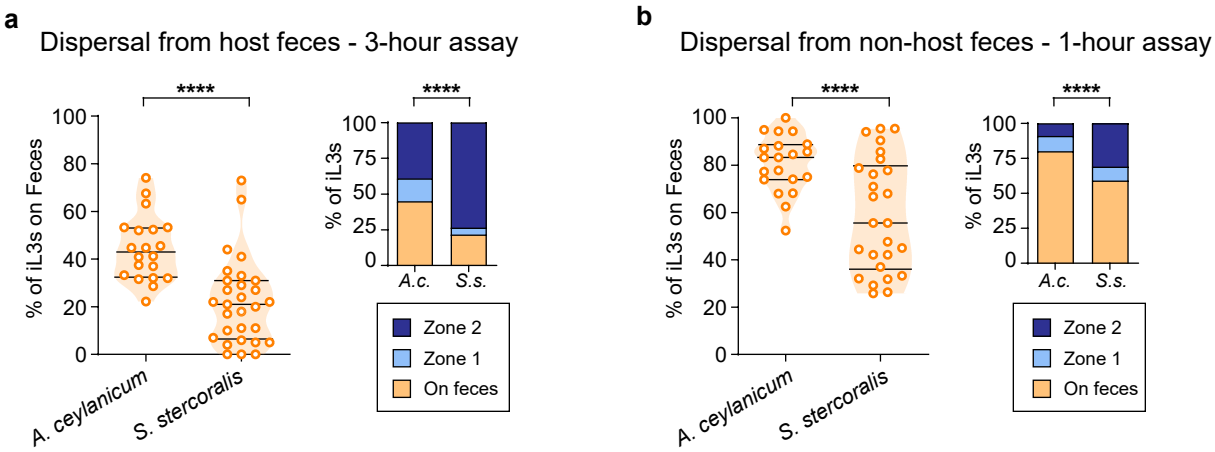

Fig. S7. *S. stercoralis* shows increased dispersal behavior relative to *A. ceylanicum*. a. Dispersal from host feces in a 3-hour fecal dispersal assay. Left, the percentage of iL3s remaining on host feces (hamster feces for *A. ceylanicum* and gerbil feces for *S. stercoralis*) at the end of the 3-hour fecal dispersal assay for *A. ceylanicum* and *S. stercoralis*. *S. stercoralis* iL3s disperse off host feces more than *A. ceylanicum* iL3s. ****P<0.0001, Mann-Whitney test. n = 20 trials for *A. ceylanicum* and 29 trials for *S. stercoralis*. Each dot represents an individual fecal dispersal assay. Lines indicate medians and interquartile ranges. Right, the percentage of iL3s in each zone at the end of the 3-hour fecal dispersal assay. The overall distribution of iL3s differed between species. ****P<0.0001, chi-squared test. In addition, the number of iL3s on feces, in zone 1, and in zone 2 all differed significantly between *A. ceylanicum* and *S. stercoralis* iL3s (P<0.001, Fisher's exact test with Bonferroni correction). **b.** Dispersal from non-host feces in a 1-hour fecal dispersal assay. Left, the percentage of iL3s remaining on non-host feces (rat feces for both *A. ceylanicum* and *S. stercoralis*) at the end of the 1-hour fecal dispersal assay for *A. ceylanicum* and *S. stercoralis*. *S. stercoralis* iL3s disperse off non-host feces more than *A. ceylanicum* iL3s. ****P<0.0001, Mann-Whitney test. n = 20 trials for *A. ceylanicum* and 26 trials for *S. stercoralis*. Each dot represents an individual fecal dispersal assay. Lines indicate medians and interquartile ranges. Right, the percentage of iL3s in each zone at the end of the 1-hour fecal dispersal assay. The overall distribution of iL3s differed between species. ****P<0.0001, chi-squared test. In addition, the number of iL3s on feces and in zone 2 differed significantly between *A. ceylanicum* and *S. stercoralis* iL3s (P<0.001, Fisher's exact test with Bonferroni correction).

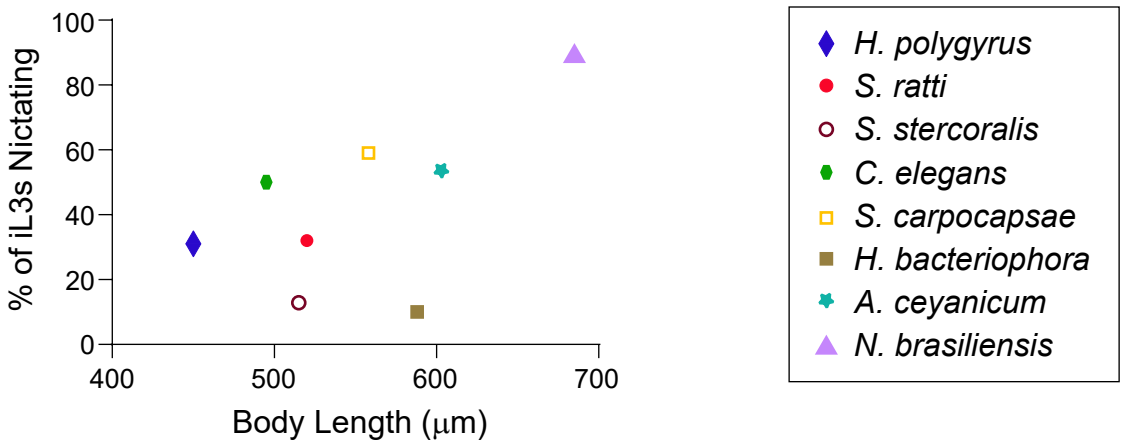

Fig. S8. Nictation frequency does not correlate with nematode body length. Graph shows the average body lengths and nictation frequencies for 8 nematode species (*Caenorhabditis elegans*, *Steinernema carpocapsae*, *Heterorhabditis bacteriophora*, *Strongyloides stercoralis*, *Strongyloides ratti*, *Nippostrongylus brasiliensis*, *Heligmosomoides polygyrus*, and *Ancylostoma ceylanicum*). No significant correlation between body length and nictation frequency was observed (Pearson $r^2 = 0.342$, $P = 0.128$). Body length measurements are for the dauer (*Caenorhabditis elegans*), infective juvenile (*Heterorhabditis bacteriophora* and *Steinernema carpocapsae*), or iL3 (all other species) life stage. Average body lengths for *Strongyloides stercoralis*, *Strongyloides ratti*, and *Ancylostoma ceylanicum* were calculated to be 515, 520, and 603 μm, respectively (n = 11-13 iL3s measured per species). Average body length data for the other species are from Adams and Nguyen, 2002; Camberis *et al.*, 2003; and Cassada and Russell, 1975 (22-24). Nictation frequencies for *Strongyloides stercoralis* and *Ancylostoma ceylanicum* are from Fig. 3. The nictation frequency for *Caenorhabditis elegans* dauers (Hawaii strain) was calculated to be 50% (n = 22 worms). The nictation frequencies for all other species are from Castelletto *et al.*, 2014 and Ruiz *et al.,* 2017 (2, 7).

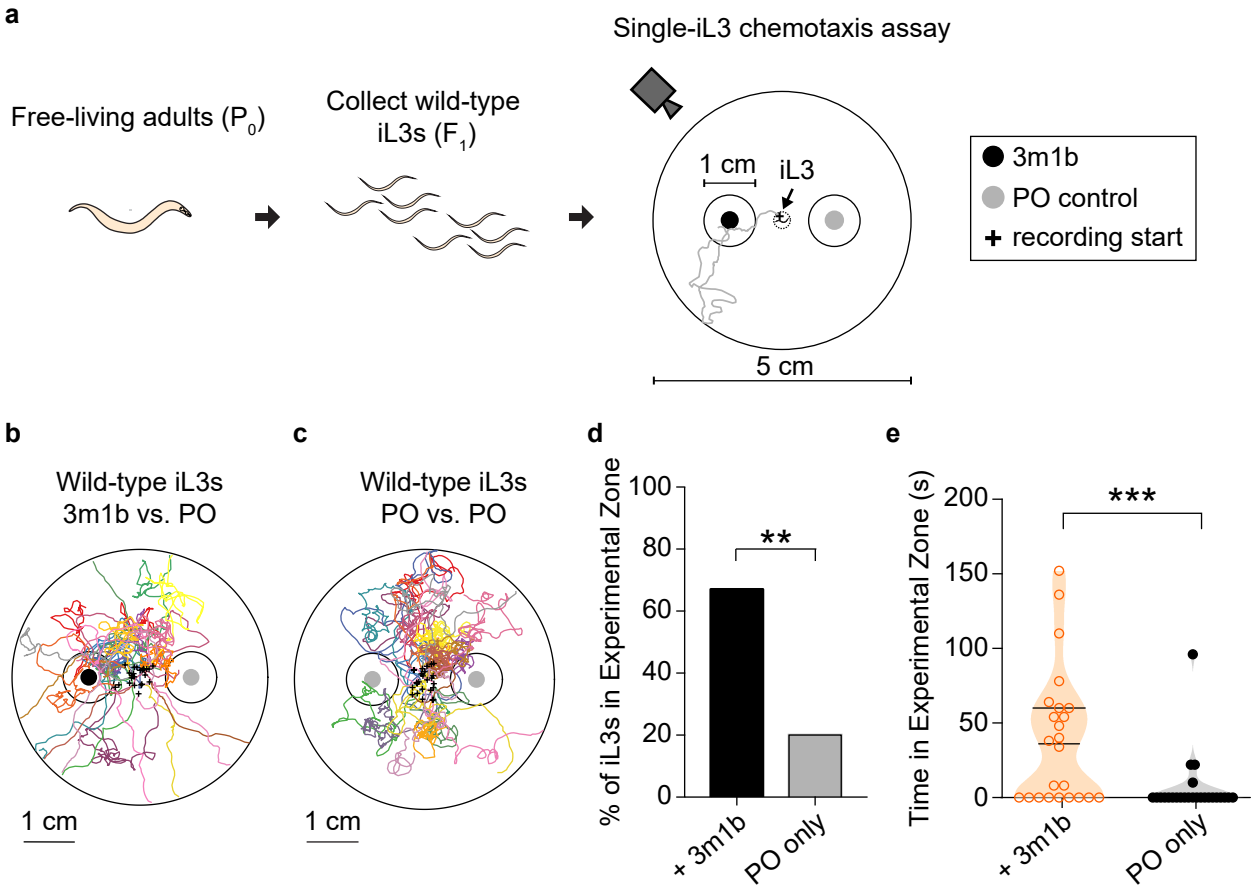

Fig. S9. *S. stercoralis* wild-type iL3s navigate toward the host odorant 3-methyl-1-butanol. a. Schematic for isolating *S. stercoralis* iL3s for single-iL3 chemotaxis assays. *S. stercoralis* free-living adults were allowed to mate on fecal-charcoal plates and populations of wild-type iL3 progeny were collected using a Baermann apparatus. Individual iL3s were then live-tracked in a chemotaxis assay where the iL3 could crawl freely on an agar surface in an odorant gradient. Black dot = placement area of a 5 μL drop of a 1:10 dilution of the attractive odorant 3-methyl-1-butanol (3m1b) in paraffin oil; grey dot = placement area of a 5 μL drop of paraffin oil control (PO); black circles around the dots = the experimental or control zones surrounding the 3m1b or PO, respectively. Grey line = hypothetical reconstruction of the migratory path of an iL3 in the chemotaxis assay; the plus sign indicates the starting position of the iL3. **b, c.** Tracks of wild-type iL3s migrating for approximately 6 minutes, or until the iL3s left the 5 cm assay arena, in a 3m1b odorant gradient (**b**) or in a control assay where PO was added to both zones (**c**). For the PO control assays, one of the zones was arbitrarily designated the experimental zone. Each colored line indicates the migration of an independently tested iL3; the plus signs indicate the starting positions of the iL3s. Black dots, grey dots, and black circles are as defined above. **d.** The percentage of wild-type iL3s entering the experimental zone for either the 3m1b odorant gradient assay or the PO-only control assay. A larger percentage of iL3s enter the experimental zone when 3m1b is present. ***P*<0.01, Fisher's exact test. **e.** The time spent by each iL3 in the experimental zone for either the 3m1b odorant gradient assay or the PO-only control assay. iL3s spend more time in the experimental zone when 3m1b is present. ****P*<0.001, Mann-Whitney test. n = 24-25 iL3s for each assay condition in **d**-**e**.

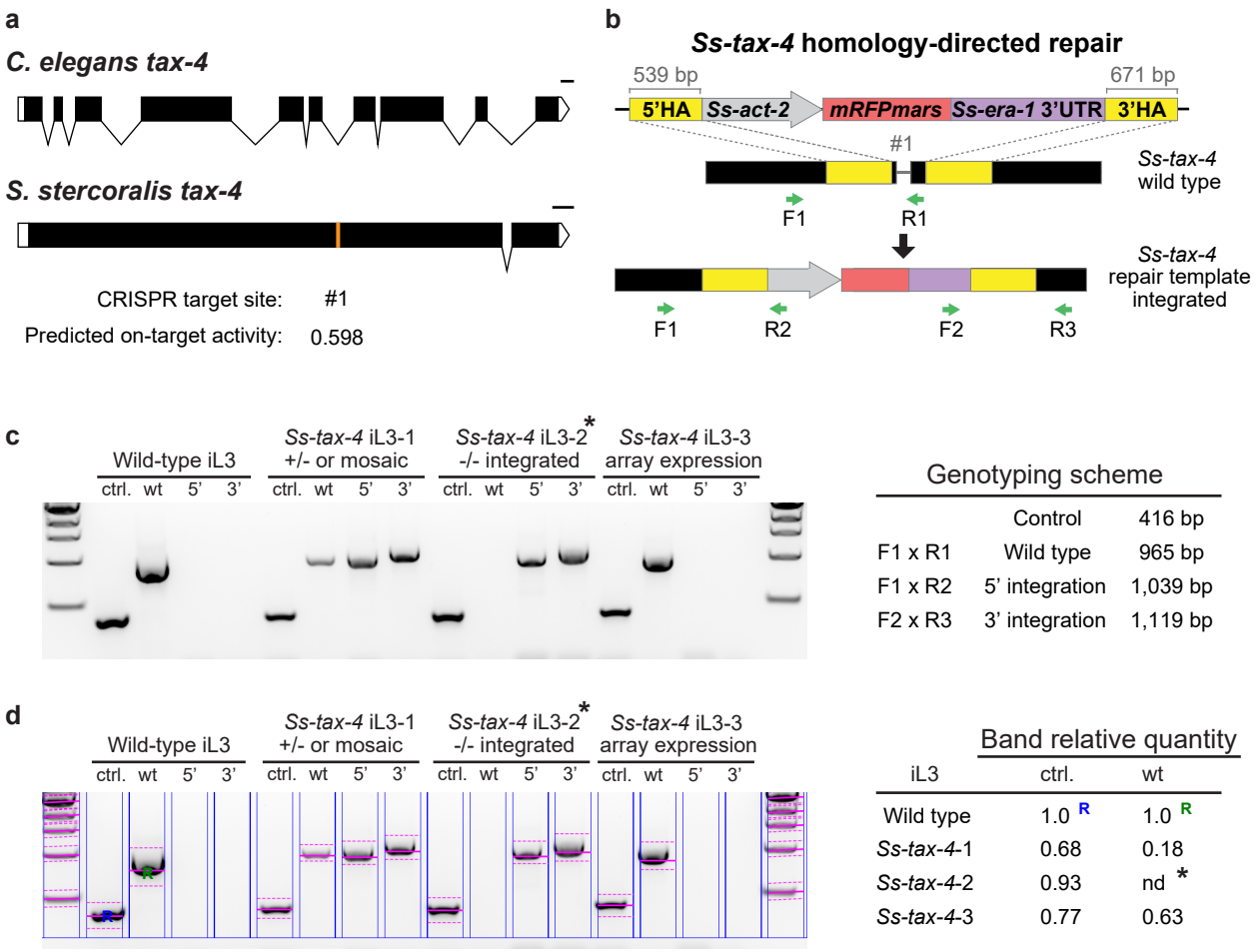

Fig. S10. Strategy for CRISPR/Cas9-mediated targeted mutagenesis of *Ss-tax-4* and genotyping for homology-directed repair (HDR). a. The *C. elegans* and *S. stercoralis tax-4* genes. The *Ss-tax-4* CRISPR target site and predicted on-target activity score is indicated (orange line) (10, 11). Scale bars = 100 bp. **b.** Homology-directed repair (HDR) strategy for *Ss-tax-4*. iL3s expressing *mRFPmars* along the full nematode body wall were selected as integration candidates and genotyped using the PCR primer sets indicated (10, 11). HA = homology arm. **c.** Left, representative gel and inferred genotypes of a wild-type iL3 and three *mRFPmars*-expressing F_1 iL3s collected from *Ss-tax-4* CRISPR-injected adults. gDNA from each iL3 was evenly divided into four reactions: ctrl. = reaction amplifying 416 bp of the first exon of the *Ss-act-2* gene to confirm successful gDNA isolation; wt = reaction amplifying the *Ss-tax-4* wild-type CRISPR locus where primer R1 overlaps the predicted cut site; 5' = reaction for HDR at the 5' border of the integrated cassette; 3' = reaction for HDR at the 3' border of the integrated cassette. 5' and 3' integration primer pairs amplify only following successful integration of *Ss-act-2::mRFPmars* into the *Ss-tax-4* target locus. For iL3 genotypes: array expression = *mRFPmars*-expressing iL3 that showed no evidence of repair template integration; +/- or mosaic = *mRFPmars*-expressing iL3 that showed integration but also showed wild-type DNA remaining at the target locus; -/- integrated = iL3s containing an *Ss-tax-4* homozygous disruption (asterisk) showing 5' and 3' integration and no amplicon for the wild-type locus. Right, summary of the PCR-genotyping scheme and predicted amplicon sizes. Size markers = 3 kb, 2 kb, 1.5 kb, 1 kb, and 500 bp from top to bottom. Primer pairs used for genotyping are shown in *SI Appendix,* Table S4. **d.** Automated detection of PCR amplicons and relative quantification of bands. The relative amount of DNA for each *mRFPmars*-expressing F_1 iL3 was quantified using the wild-type control as a reference. Blue "R" = reference band for quantification of the *act-2* control reactions; green "R" = reference band for quantification of the *Ss-tax-4* wild-type locus reactions; nd * = no PCR amplicon was detected, thus this iL3 was considered to have an *Ss-tax-4* homozygous disruption.

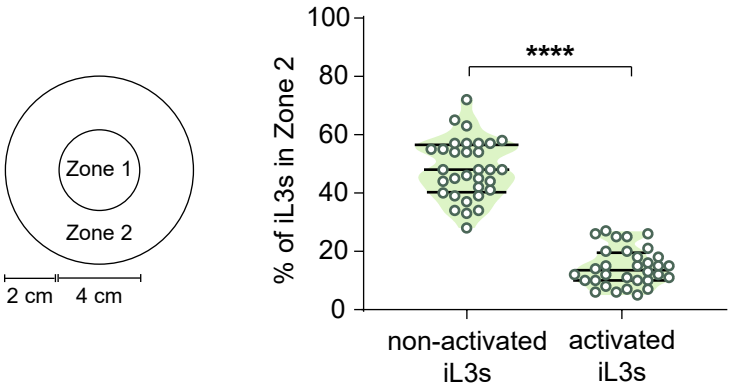

Fig. S11. *S. stercoralis* iL3*s* that have activated show decreased dispersal behavior relative to *S. stercoralis* iL3s that have not activated. Dispersal from the center zone of a 10-cm plate was measured for iL3s subjected to either activation conditions (37°C, DMEM, 5% CO_2) or control conditions (room temperature, BU saline, no applied CO_2). Left, diagram of the dispersal assay. iL3s were placed in the center of a 10-cm plate and then allowed to disperse at room temperature for 1 hour. The percentage of iL3s that had crawled out of Zone 1 and into Zone 2 was then quantified. Right, the iL3s subjected to activation conditions ("activated iL3s") dispersed less than the iL3s subjected to control conditions ("non-activated iL3s"). ****P<0.0001, Welch's t-test. n = 32 trials for each condition. Each dot represents an individual dispersal assay. Lines show medians and interquartile ranges.

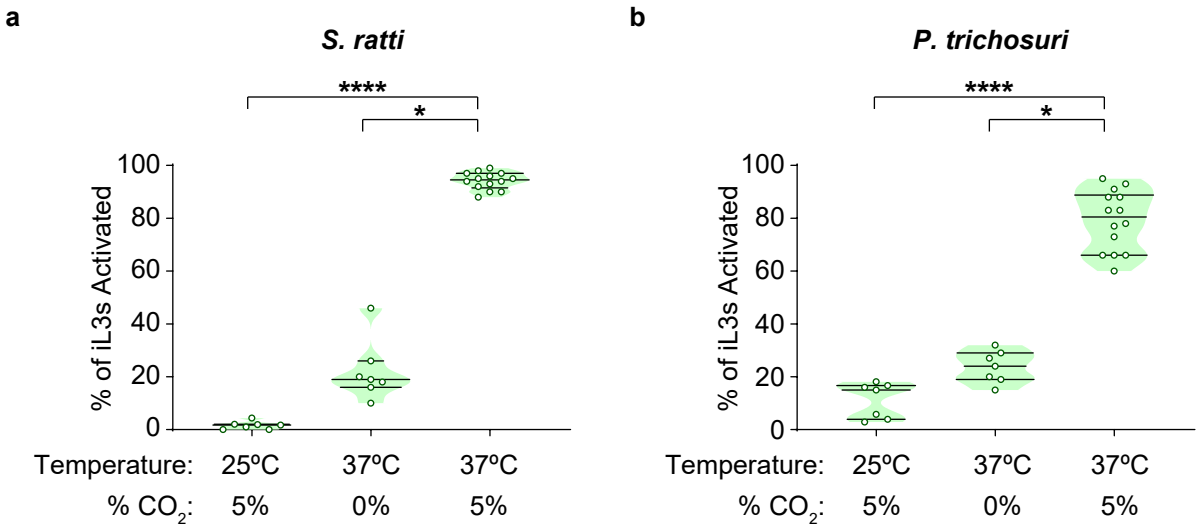

Fig S12. *In vitro* activation of *S. ratti* and *P. trichosuri* iL3s. a. Heat and CO_2 are required for activation of *S. ratti* iL3s. **P*<0.05, *****P*<0.0001, Kruskal-Wallis test with Dunn's post-test. n = 7-14 trials per condition. **b.** Heat and CO_2 are required for activation of *P. trichosuri* iL3s. **P*<0.05, *****P*<0.0001, Kruskal-Wallis test with Dunn's post-test. n = 7-14 trials per condition. For **a** and **b**, % of iL3s activated = # FITC-positive iL3s / total # iL3s scored. Green dots = % activation for each trial, with approximately 100 iL3s scored per trial. Lines show medians and interquartile ranges.

Supplementary Tables

Table S1. Human-associated odorants tested. Superscripts denote the control used in chemotaxis assays and the diluent used to make 1:10 odorant dilutions as described in the methods (p = paraffin oil, w = ddH_2O, e = ethanol). Odorant sources are not exhaustive. Animal feces were also tested and were diluted in ddH_2O.

Odorant	Class	Human Source	CAS #	References
3-methyl-1-butanol$^{(p)}$	alcohol	skin, sweat, feces, saliva	123-51-3	(25-29)
1-heptanol$^{(p)}$	alcohol	sweat, feces, hair, scalp	111-70-6	(25, 26, 29, 30)
1-octanol$^{(p)}$	alcohol	sweat, feces, hair, scalp, urine	111-87-5	(25, 26, 28-30)
1-nonanol$^{(p)}$	alcohol	sweat, feces, hair, scalp	143-08-8	(25, 26, 28-30)
farnesol$^{(p)}$	alcohol	sebum	4602-84-0	(31)
3-heptanol$^{(p)}$	alcohol	skin, feces	589-82-2	(29, 32)
2-phenylethanol$^{(e)}$	alcohol	feces, urine	60-12-8	(29, 33)
isovaleric acid$^{(p)}$	acid	skin, sweat, feces, saliva, urine	503-74-2	(25-27, 29, 34-36)
acetic acid$^{(w)}$	acid	skin, sweat, feces, hair, scalp, breath, saliva	64-19-7	(25, 28-30, 33-35, 37-40)
hexanoic acid$^{(p)}$	acid	skin, sweat, feces, saliva, urine	142-62-1	(25, 26, 29, 34, 36-38)
decyl acetate$^{(p)}$	acetate	feces	112-17-4	(28)
3-octanone$^{(p)}$	ketone	feces, saliva	106-68-3	(26, 29)
β-myrcene$^{(p)}$	hydrocarbon	feces	123-35-3	(26)
tetradecane$^{(p)}$	hydrocarbon	skin, feces, hair, scalp	629-59-4	(26, 29, 30, 37)
pentadecane$^{(p)}$	hydrocarbon	skin, feces, hair, scalp	629-62-9	(29, 30, 37)
p-cresol$^{(p)}$	aromatic	skin, feces, urine	106-44-5	(26, 29, 33, 38, 40, 41)
α-terpinene$^{(p)}$	aromatic	urine, saliva	99-86-5	(29, 42)
skatole$^{(e)}$	aromatic heterocyclic	feces, urine	83-34-1	(29, 33, 41, 43)
indole$^{(e)}$	aromatic heterocyclic	skin, sweat, feces, urine	120-72-9	(25, 26, 28, 29, 33, 37, 41, 43, 44)
α-pinene$^{(p)}$	bicyclic monoterpene	feces, breath	7785-70-8	(26, 29, 45)
3-carene$^{(p)}$	bicyclic monoterpene	feces, breath	498-15-7	(26, 29, 45)

Table S2. Summary of *Ss-tax-4* microinjections, F_1 iL3 screening, and genotyping of *Ss-tax-4* knockout iL3s. Percentages in the last two columns were calculated based on the number of red iL3s genotyped by PCR. na = not available; total progeny counts were not recorded for this experiment. The bottom row shows the totals from all experiments.

# free-living adults injected	# iL3s screened	# red iL3s collected	# red iL3s genotyped	# repair-template integrated (%)	# *Ss-tax-4* knockouts (%)
20	na	40	25	19 (76%)	8 (32%)
15	333	12	12	6 (50%)	3 (25%)
17	680	6	6	4 (66%)	3 (50%)
30	487	18	18	14 (77%)	6 (33%)
23	160	12	12	9 (75%)	4 (33%)
25	256	10	10	8 (80%)	5 (50%)
24	891	12	12	12 (100%)	9 (75%)
154	**2,807**	**110**	**95**	**72 (76%)**	**38 (40%)**

Table S3. Plasmids used in this study. pPV540 was modified from pPV402, which is described in Shao *et al.,* 2012 (46). pEY11 was modified from pAJ50, which is described in Junio *et al.,* 2008 (16). pMLC47 was generated in Gang *et al.,* 2017 (10). The plasmids were used previously in Bryant *et al.,* 2018 (11).

Construct	Description	Backbone
pPV540 (*Sr-eef-1A$_p$::Cas9::Ss-era-1* 3'UTR)	*Strongyloides* codon-optimized Cas9	pPV402
pMLC47 (*Sr-U6$_p$::Ss-tax-4-sgRNA::Sr-U6* 3'UTR)	sgRNA for *Ss-tax-4*	pUC57-Kan
pEY11 (5'HA*::Ss-act-2$_p$::mRFPmars::Ss-era-1* 3'UTR::3'HA)	HDR construct for *Ss-tax-4*	pAJ50

Table S4. Oligonucleotides used in this study. F = forward primer; R = reverse primer.

Oligonucleotide set (5' to 3')	Description	Size (bp)	Notes
F: TGGTTATCCTCTGACTTGATAGCTG R: TCAATATTTTGTACTGGACCAGGAAC	*Ss-tax-4* 5' homology arm in pEY11	539 bp	
F: TCGATGATTTCCAATATGTCTGCTG R: TCCACTGTATTTTGTTCTTCTGGTG	*Ss-tax-4* 3' homology arm in pEY11	671 bp	
F: GTATTCCCTTCTATTGTTGGAAGACC R: CCTTCATAGATTGGTACAGTGTGAG	*Ss-act-2* exon 1 gDNA control	416 bp	Control in Figure S10
F: TTCTAATTCTTCAAAAATGCCAAAGTCC R: TTGTAGCAAAAATTAAAACCCCACC	*Ss-tax-4* wild-type locus	965 bp	F1 x R1 in Figure S10
F: TTCTAATTCTTCAAAAATGCCAAAGTCC R: CGAGGTACCTCTTTTCCACACTT	*Ss-tax-4* 5' integration	1,039 bp	F1 x R2 in Figure S10
F: AAACAGAAACAGATTGGGTCTCT R: AGGTTTGTAAGTCAATGCATCTTGG	*Ss-tax-4* 3' integration	1,119 bp	F2 x R3 in Figure S10

Supplementary Movie Legends

Movie S1. An *S. stercoralis* wild-type iL3 emerging from a ~1 μL droplet of ddH_2O and crawling toward 3-methyl-1-butanol (3m1b). Black dot = placement area of a 5 μL drop of a 1:10 dilution of 3m1b; grey dot = placement area of a 5 μL drop of paraffin oil control. Inner circles = experimental zones for the odorant and control; outer circle = arena for the single-iL3 chemotaxis assay. Scale bar = 1 cm. Movie speed is 60x.

Movie S2. An *S. stercoralis* wild-type iL3 emerging from a ~1 μL droplet of ddH_2O crawling in a paraffin oil control assay. Grey dots = placement areas of 5 μL drops of paraffin oil control. Inner circles = experimental zones; outer circle = arena for the single-iL3 chemotaxis assay. Scale bar = 1 cm. Movie speed is 60x.

Movie S3. A no-Cas9-control iL3 emerging from a ~1 μL droplet of ddH_2O and crawling toward 3-methyl-1-butanol (3m1b). Black dot = placement area of a 5 μL drop of a 1:10 dilution of 3m1b; grey dot = placement area of a 5 μL drop of paraffin oil control. Inner circles = experimental zones for the odorant and control; outer circle = arena for the single-iL3 chemotaxis assay. Scale bar = 1 cm. Movie speed is 60x.

Movie S4. An *Ss-tax-4* iL3 emerging from a ~1 μL droplet of ddH_2O that fails to navigate toward 3-methyl-1-butanol (3m1b). Black dot = placement area of a 5 μL drop of a 1:10 dilution of 3m1b; grey dot = placement area of a 5 μL drop of paraffin oil control. Inner circles = experimental zones for the odorant and control; outer circle = arena for the single-iL3 chemotaxis assay. Scale bar = 1 cm. Movie speed is 60x.

SI References

1. Lok JB (2007) *Strongyloides stercoralis:* a model for translational research on parasitic nematode biology. In WormBook, www.wormbook.org, 1-18.
2. Castelletto ML*, et al.* (2014) Diverse host-seeking behaviors of skin-penetrating nematodes. *PLoS Pathog* 10:e1004305.
3. Grant WN*, et al.* (2006) *Parastrongyloides trichosuri,* a nematode parasite of mammals that is uniquely suited to genetic analysis. *Int J Parasitol* 36:453-466.
4. Stasiuk SJ, Scott MJ, & Grant WN (2012) Developmental plasticity and the evolution of parasitism in an unusual nematode, *Parastrongyloides trichosuri*. *Evodevo* 3:1.
5. Brenner S (1974) The genetics of *Caenorhabditis elegans*. *Genetics* 77:71-94.
6. Hawdon JM & Schad GA (1991) Long-term storage of hookworm infective larvae in buffered saline solution maintains larval responsiveness to host signals. *J Helm Soc Wash* 58:140-142.
7. Ruiz F, Castelletto ML, Gang SS, & Hallem EA (2017) Experience-dependent olfactory behaviors of the parasitic nematode *Heligmosomoides polygyrus*. *PLoS Pathog* 13:e1006709.
8. Bargmann CI, Hartwieg E, & Horvitz HR (1993) Odorant-selective genes and neurons mediate olfaction in *C. elegans*. *Cell* 74:515-527.
9. Lee H*, et al.* (2012) Nictation, a dispersal behavior of the nematode *Caenorhabditis elegans,* is regulated by IL2 neurons. *Nat Neurosci* 15:107-112.
10. Gang SS*, et al.* (2017) Targeted mutagenesis in a human-parasitic nematode. *PLoS Pathog* 13:e1006675.
11. Bryant AS*, et al.* (2018) A critical role for thermosensation in host seeking by skin-penetrating nematodes. *Curr Biol* 28:2338-2347.
12. Hunt VL*, et al.* (2016) The genomic basis of parasitism in the *Strongyloides* clade of nematodes. *Nat Genet* 48:299-307.
13. Kearse M*, et al.* (2012) Geneious Basic: an integrated and extendable desktop software platform for the organization and analysis of sequence data. *Bioinformatics* 28:1647-1649.
14. Doench JG*, et al.* (2014) Rational design of highly active sgRNAs for CRISPR-Cas9-mediated gene inactivation. *Nat Biotechnol* 32:1262-1267.
15. Farboud B & Meyer BJ (2015) Dramatic enhancement of genome editing by CRISPR/Cas9 through improved guide RNA design. *Genetics* 199:959-971.
16. Junio AB*, et al.* (2008) *Strongyloides stercoralis:* cell- and tissue-specific transgene expression and co-transformation with vector constructs incorporating a common multifunctional 3' UTR. *Exp Parasitol* 118:253-265.
17. Mello C & Fire A (1995) DNA transformation. *Methods Cell Biol* 48:451-482.
18. Ashton FT, Zhu X, Boston R, Lok JB, & Schad GA (2007) *Strongyloides stercoralis*: amphidial neuron pair ASJ triggers significant resumption of development by infective larvae under host-mimicking *in vitro* conditions. *Exp Parasitol* 115:92-97.

19. Faul F, Erdfelder E, Lang AG, & Buchner A (2007) G*Power 3: a flexible statistical power analysis program for the social, behavioral, and biomedical sciences. *Behav Res Methods* 39:175-191.

20. Babicki S*, et al.* (2016) Heatmapper: web-enabled heat mapping for all. *Nucleic Acids Res* 44:W147-W153.

21. Hammer Ø, Harper DAT, & Ryan PD (2001) PAST: Paleontological statistics software package for education and data analysis. *Palaeontol Electronica* 4:1-9.

22. Adams BJ & Nguyen KB (2002) Taxonomy and systematics. *Entomopathogenic Nematology*, Gaugler R, Ed. (New York), CABI Publishing, pp 1-33.

23. Camberis M, Le Gros G, & Urban J (2003) Animal model of *Nippostrongylus brasiliensis* and *Heligmosomoides polygyrus. Curr. Protoc. Immunol.* 19:19.12.11–19.12.27.

24. Cassada RC & Russell RL (1975) The dauerlarva, a post-embryonic developmental variant of the nematode *Caenorhabditis elegans*. *Dev Biol* 46:326-342.

25. Meijerink J*, et al.* (2000) Identification of olfactory stimulants for *Anopheles gambiae* from human sweat samples. *J Chem Ecol* 26:1367-1382.

26. Garner CE*, et al.* (2007) Volatile organic compounds from feces and their potential for diagnosis of gastrointestinal disease. *FASEB J* 21:1675-1688.

27. Verhulst NO*, et al.* (2009) Cultured skin microbiota attracts malaria mosquitoes. *Malaria J* 8:302.

28. Tait E, Perry JD, Stanforth SP, & Dean JR (2014) Use of volatile compounds as a diagnostic tool for the detection of pathogenic bacteria. *Trends Analyt Chem* 53:117-125.

29. Wishart DS*, et al.* (2018) HMDB 4.0: the human metabolome database for 2018. *Nucleic Acids Res* 46:D608-D617.

30. Goetz N, Kaba G, Good D, Hussler G, & Bore P (1988) Detection and identification of volatile compounds evolved from human hair and scalp using headspace gas chromatography. *J Soc Cosmet Chem* 39:1-13.

31. Nicolaides N (1965) Skin lipids. IV. Biochemistry and function. *J Am Oil Chem Soc* 42:708-712.

32. Smallegange RC*, et al.* (2012) Identification of candidate volatiles that affect the behavioural response of the malaria mosquito *Anopheles gambiae sensu stricto* to an active kairomone blend: laboratory and semi-field assays. *Physiol Entomol* 37:60-71.

33. Starkenmann C (2017) Analysis and chemistry of human odors. *Periodical Analysis and chemistry of human odors,* Buettner A, Ed. (Cham), Springer, pp 921-936.

34. Ara K*, et al.* (2006) Foot odor due to microbial metabolism and its control. *Can J Microbiol* 52:357-364.

35. Caroprese A, Gabbanini S, Beltramini C, Lucchi E, & Valgimigli L (2009) HS-SPME-GC-MS analysis of body odor to test the efficacy of foot deodorant formulations. *Skin Res Technol* 15:503-510.

36. Cork A & Park KC (1996) Identification of electrophysiologically-active compounds for the malaria mosquito, *Anopheles gambiae*, in human sweat extracts. *Med Vet Entomol* 10:269-276.

37. Bernier UR, Kline DL, Barnard DR, Schreck CE, & Yost RA (2000) Analysis of human skin emanations by gas chromatography/mass spectrometry. 2. Identification of volatile compounds that are candidate attractants for the yellow fever mosquito (*Aedes aegypti*). *Anal Chem* 72:747-756.

38. Gallagher M*, et al.* (2008) Analyses of volatile organic compounds from human skin. *Br J Dermatol* 159:780-791.

39. Phillips M*, et al.* (1999) Variation in volatile organic compounds in the breath of normal humans. *J Chromatogr B Biomed Sci Appl* 729:75-88.

40. De Preter V, Van Staeyen G, Esser D, Rutgeerts P, & Verbeke K (2009) Development of a screening method to determine the pattern of fermentation metabolites in faecal samples using on-line purge-and-trap gas chromatographic-mass spectrometric analysis. *J Chromatogr A* 1216:1476-1483.

41. Chappuis CJ, Niclass Y, Vuilleumier C, & Starkenmann C (2015) Quantitative headspace analysis of selected odorants from latrines in Africa and India. *Environ Sci Technol* 49:6134-6140.

42. Wahl HG, Hoffmann A, Luft D, & Liebich HM (1999) Analysis of volatile organic compounds in human urine by headspace gas chromatography-mass spectrometry with a multipurpose sampler. *J Chromatogr A* 847:117-125.

43. Moore JG, Jessop LD, & Osborne DN (1987) Gas-chromatographic and mass-spectrometric analysis of the odor of human feces. *Gastroenterology* 93:1321-1329.

44. Syed Z & Leal WS (2009) Acute olfactory response of *Culex* mosquitoes to a human- and bird-derived attractant. *Proc Natl Acad Sci USA* 106:18803-18808.

45. Mochalski P*, et al.* (2013) Blood and breath levels of selected volatile organic compounds in healthy volunteers. *Analyst* 138:2134-2145.

46. Shao H*, et al.* (2012) Transposon-mediated chromosomal integration of transgenes in the parasitic nematode *Strongyloides ratti* and establishment of stable transgenic lines. *PLoS Pathog* 8:e1002871.